

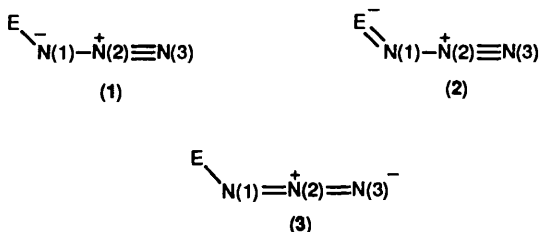
## Synthesis and Characterization of Transition-metal-substituted Germanium and Tin Azides: X-Ray Crystal Structures of $[\{\text{Fe}(\text{CO})_2(\text{cp})\}_2\text{E}(\text{N}_3)_2]$ ( $\text{cp} = \eta\text{-C}_5\text{H}_5$ , $\text{E} = \text{Ge}$ or $\text{Sn}$ )<sup>†</sup>

Mark J. Hampden-Smith,\* Deqing Lei, and Eileen N. Duesler

Department of Chemistry and Center for Micro-Engineered Ceramics, University of New Mexico, Albuquerque, NM 87131, U.S.A.

Treatment of acetonitrile solutions of  $[\{\text{Fe}(\text{CO})_2(\text{cp})\}_2\text{EX}_2]$  ( $\text{cp} = \eta\text{-C}_5\text{H}_5$ ;  $\text{E} = \text{Ge}$ ,  $\text{X} = \text{Br}$ ;  $\text{E} = \text{Sn}$ ,  $\text{X} = \text{Cl}$ ) with an excess of sodium azide affords the compounds  $[\{\text{Fe}(\text{CO})_2(\text{cp})\}_2\text{E}(\text{N}_3)_2]$  ( $\text{E} = \text{Ge}$  or  $\text{Sn}$ ). X-Ray crystallographic analyses of these compounds show that the Group 14 atom has a distorted-tetrahedral environment, with enlarged Fe–E–Fe angles and reduced N–E–N angles. Contributions from various resonance forms of the azide ligand are discussed, based on the solid-state data, and are compared to expectations based on solid-state and solution  $\nu_{\text{asym}}(\text{N}_3)$  and  $\nu(\text{CO})$  i.r. stretching frequencies.

The bonding in organometallic azides of the Group 14 elements can be described by any of the three canonical forms<sup>1</sup> (1)–(3) shown below. Single-crystal X-ray diffraction studies have



shown that organic azides (*e.g.*  $\text{E} = sp^3$  or  $sp^2$ -hybridized carbon fragment) adopt a canonical form more analogous to (1) than to (2) or (3).<sup>2</sup> They also exhibit a characteristic  $\nu(\text{N}_3)$  asymmetric stretching frequency of *ca.*  $2100 \pm 15 \text{ cm}^{-1}$ . Thayer<sup>3</sup> has correlated the structure and reactivity with asymmetric  $\nu(\text{N}_3)$  stretching frequency as a means of classifying organometallic azides. Two types were identified: Type A, which includes the azides of B, Si, Ge, P, and As, which have  $\nu_{\text{asym}}(\text{N}_3) > \nu_{\text{sym}}(\text{N}_3)$  of organic azides, and Type B, which includes azides of Sn, Pb, Hg, Sb, and Ti, which have  $\nu_{\text{asym}}(\text{N}_3) < \nu_{\text{sym}}(\text{N}_3)$  of organic azides. These trends can be correlated with contributions from different resonance forms of the azide ligands, with both (1) and (2) making a major contribution to Type A azides and (3) making the major contribution to Type B azides. West and co-workers<sup>4</sup> have recently demonstrated, however, that the azide ligand in two silyl azide derivatives, azidotris(2,4,6-trimethylphenyl)silane, (4), and azido-2,2-diphenyl-2-t-butyl-1,1-bis(2,4,6-trimethylphenyl)disilane, (5), appear to adopt a higher contribution from canonical form (3), by comparison of the N(1)–N(2) and N(2)–N(3) distances. This is in contrast to the expectations based on their i.r. stretching frequencies ( $2140$  and  $2120 \text{ cm}^{-1}$ , respectively).<sup>5</sup> Structural studies of organometallic azides of the lower members of Group 14 are fairly sparse. Two germanium azides have been structurally characterized, but possess distorted germanium co-ordination environments.<sup>6,7</sup> Structurally characterized tin azides exhibit intermolecular association involving the azide ligand.<sup>8,9</sup> As part of our studies of organotransition-metal Group 14 chemistry,<sup>10</sup> we now report the synthesis and characterization of two new germanium and tin diazide species.

### Experimental

(a) *Synthesis*.—All manipulations were carried out under an atmosphere of dry ( $4 \text{ \AA}$  molecular sieves), deoxygenated ( $\text{MnO}$ ) nitrogen.<sup>11</sup> Hydrocarbon solvents were dried and distilled from sodium diphenylketyl and stored under nitrogen over molecular sieves. Acetonitrile was dried with  $\text{CaH}_2$  and distilled from  $\text{P}_2\text{O}_5$ .<sup>12</sup> Deuteriated n.m.r. solvents were dried over  $4 \text{ \AA}$  molecular sieves and stored under nitrogen. The starting materials,  $[\{\text{Fe}(\text{CO})_2(\text{cp})\}_2\text{SnCl}_2]$  and  $[\{\text{Fe}(\text{CO})_2(\text{cp})\}_2\text{GeBr}_2]$  ( $\text{cp} = \eta\text{-C}_5\text{H}_5$ ), were prepared by the reaction of  $\text{SnCl}_2$  (Aldrich) and  $\text{GeBr}_2$  with  $[\{\text{Fe}(\text{CO})_2(\text{cp})\}_2]$  (Aldrich) using the method of Bonati and Wilkinson.<sup>13</sup> Germanium bromide was prepared by bromination of powdered germanium (Johnson Matthey) metal at  $400 \text{ }^\circ\text{C}$ .<sup>14</sup>

N.m.r. spectra were recorded on a Bruker AC-250 spectrometer. Proton chemical shifts were referenced to the protio impurity of the deuteriated solvent, and carbon-13 chemical shifts to the central  $^{13}\text{C}$  n.m.r. resonance of the deuteriated solvent. Tin-119 n.m.r. data were referenced to external  $\text{SnMe}_4$  using the low field = positive sign convention. I.r. spectra were recorded on a Perkin-Elmer 1620 FTIR spectrometer. Elemental analyses were performed by Oneida Research Services.

The compounds  $[\{\text{Fe}(\text{CO})_2(\text{cp})\}_2\text{E}(\text{N}_3)_2]$  ( $\text{E} = \text{Ge}$  or  $\text{Sn}$ ) were prepared by similar methods. The procedure for the germanium derivative is described in detail. Sodium azide ( $0.22 \text{ g}$ ,  $3.4 \text{ mmol}$ ) was dissolved in acetonitrile ( $30 \text{ cm}^3$ ) and transferred, *via* canula tubing, to a flask containing  $[\{\text{Fe}(\text{CO})_2(\text{cp})\}_2\text{GeBr}_2]$  ( $0.50 \text{ g}$ ,  $0.85 \text{ mmol}$ ) dissolved in acetonitrile ( $50 \text{ cm}^3$ ). A white precipitate immediately appeared in the brown solution. After stirring for 36 h the solution was filtered and the volatile components removed *in vacuo*. Pale red-orange crystals of the product were formed while the solvent was being removed. A  $^1\text{H}$  n.m.r. spectrum of the crude residue obtained indicated the presence of a single type of cyclopentadienyl ligand. The residue was dissolved in the minimum amount of warm ( $\approx 40 \text{ }^\circ\text{C}$ ) acetonitrile and cooled to  $-30 \text{ }^\circ\text{C}$  for 12 h. During this time pale orange-yellow crystals formed and were isolated by filtration at  $0 \text{ }^\circ\text{C}$ . Analytical data for this

<sup>†</sup> Diazidobis[dicarbonyl( $\eta$ -cyclopentadienyl)ferrio]-germanium and -tin.

Supplementary data available: see Instructions for Authors, *J. Chem. Soc., Dalton Trans.*, 1990, Issue 1, pp. xix–xxii.

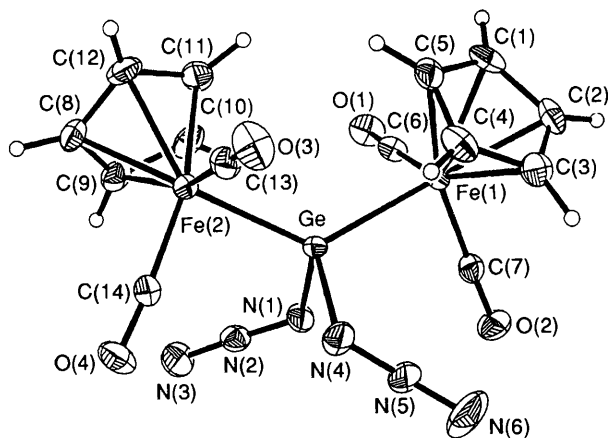


Figure 1. An ORTEP plot of compound (6) showing the atom numbering scheme

product are consistent with the empirical formula  $[\{\text{Fe}(\text{CO})_2(\text{cp})\}_2\text{Ge}(\text{N}_3)_2]$ , (6).

**Characterization data for compound (6).** I.r. (KBr disc): 2 087s, 2 065s, 2 008s, 1 962s, 1 954s, 1 430m, 1 417m, 1 332m, 1 278m, 1 264s, 1 015m, 1 006m, 857m, 843m, 631s, 602m(sh), 576s, 513m, and 404m; ( $\text{C}_6\text{D}_6$  solution)  $\nu(\text{N}_3)$  2 091, 2 073;  $\nu(\text{CO})$  2 023, 2 000, 1 969, and 1 955  $\text{cm}^{-1}$ . N.m.r. data ( $\text{C}_6\text{D}_6$ , 20 °C):  $^1\text{H}$  (250 MHz),  $\delta$  4.28 (s,  $\text{C}_5\text{H}_5$ );  $^{13}\text{C}$  (62.9 MHz);  $\delta$  212.9 (s, CO) and 83.9 p.p.m. (s,  $\text{C}_5\text{H}_5$ ) (Found: C, 32.95; H, 1.95; N, 16.65 calc. for  $\text{C}_{14}\text{H}_{10}\text{Fe}_2\text{GeN}_6\text{O}_4$ : C, 32.90%; H, 1.75; N, 16.35%).

**Characterization data for  $[\{\text{Fe}(\text{CO})_2(\text{cp})\}_2\text{Sn}(\text{N}_3)_2]$ , (7).** I.r. (KBr disc): 2 088s, 2 073s, 2 059s, 1 992s, 1 959s, 1 428m, 1 413m, 1 314m, 1 268m, 1 065w, 1 018w, 999m(sh), 857m, 626m, 517s, 512m, 455m, and 441m; ( $\text{C}_6\text{D}_6$  solution)  $\nu(\text{N}_3)$  2 075, 2 060;  $\nu(\text{CO})$  2 019, 1 997, 1 969, and 1 955  $\text{cm}^{-1}$ . N.m.r. data (20 °C):  $^1\text{H}$  [ $(\text{CD}_3)_2\text{CO}$ , 250 MHz],  $\delta$  5.30 (s,  $\text{C}_5\text{H}_5$ );  $^{13}\text{C}$  ( $\text{C}_6\text{D}_6$ , 62.9 MHz),  $\delta$  211.7 (s, CO) and 84.2 p.p.m. (s,  $\text{C}_5\text{H}_5$ );  $^{119}\text{Sn}$  ( $\text{C}_6\text{D}_6$ , 93.3 MHz),  $\delta$  +520.9 p.p.m. (Found: C, 30.5; H, 1.70; N, 14.10. Calc. for  $\text{C}_{14}\text{H}_{10}\text{Fe}_2\text{N}_6\text{O}_4\text{Sn}$ : C, 30.20; H, 1.80; N, 15.10%).

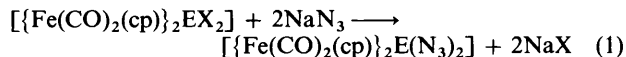
(b) **X-Ray Crystallographic Study of Compound (6).**—Orange blocks of compound (6) were grown from acetonitrile at  $-30$  °C, and the crystal selected for X-ray study was sealed in a glass capillary under nitrogen. A total of 3 517 independent reflections were measured on a Nicolet R3m/V diffractometer. The structure was solved by direct methods using SHELXTL PLUS and refined by the full-matrix least-squares method. Hydrogen-atom positions were calculated and allowed to ride on the carbon atom to which they were bonded with fixed  $U$  values. A final difference Fourier map was featureless, with the largest peak being  $0.43 \text{ e } \text{\AA}^{-3}$ . Details of the crystal data are given in Table 1, and atomic co-ordinates in Table 2. Relevant bond lengths and angles are given in Tables 3 and 4, respectively.

(c) **X-Ray Crystallographic Study of Compound (7).**—Clear orange prisms of compound (7) were grown from acetonitrile at  $-30$  °C. Data-collection and refinement techniques were analogous to those described in (b). 1 782 independent reflections were collected, and hydrogen-atom positions were calculated and allowed to ride on the carbon atom to which they were bonded with varied  $U$  values. A final difference Fourier map was featureless, with the largest peak being  $1.02 \text{ e } \text{\AA}^{-3}$ . Details of the crystal data are given in Table 1, and atomic co-ordinates and in Table 2. Relevant bond lengths and angles are given in Tables 3 and 4, respectively.

Additional material available from the Cambridge Crystallographic Data Centre comprises H-atom co-ordinates, thermal parameters, and remaining bond lengths and angles.

## Results and Discussion

The compounds  $[\{\text{Fe}(\text{CO})_2(\text{cp})\}_2\text{E}(\text{N}_3)_2]$  [E = Ge, (6); or Sn, (7)] were prepared by the metathesis reaction (1). Both have



been structurally characterized in the solid state by single-crystal X-ray diffraction. The numbering schemes are given in Figures 1 and 2, relevant bond distances and angles in Tables 3 and 4.

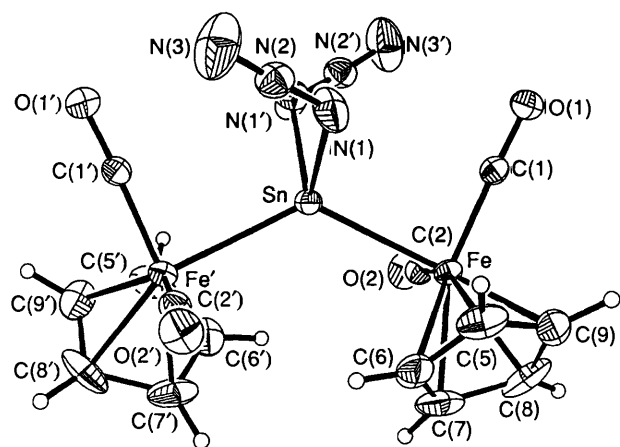
**Solid-state Structures of  $[\{\text{Fe}(\text{CO})_2(\text{cp})\}_2\text{E}(\text{N}_3)_2]$  (E = Ge or Sn).**—Compound (6) possesses no molecular symmetry in the solid state ( $C_1$ ), and the two azide ligands have different metrical parameters. The N(1)–N(2) distance [ $1.204(6) \text{ \AA}$ ] is longer than the N(2)–N(3) distance [ $1.139(7) \text{ \AA}$ ], within the limits of error of the data; therefore, this azide ligand more closely resembles canonical form (1). The N(4)–N(5) distance [ $1.178(7) \text{ \AA}$ ] is also longer than the N(5)–N(6) distance [ $1.121(10) \text{ \AA}$ ], but the difference between these distances is smaller than in the case of the other azide substituent. However, the difference of  $0.059 \text{ \AA}$  between N(4)–N(5) and N(5)–N(6) represents about six standard deviations, and as a result we conclude that this azide ligand more closely resembles canonical form (1) also. In addition, it is noteworthy that the differences in distances between N(1)–N(2) and N(4)–N(5) and between N(2)–N(3) and N(5)–N(6) are  $0.026$  and  $0.021 \text{ \AA}$ , respectively, corresponding to about three standard deviations and therefore may not be significant. Both Ge–N distances [ $1.948(4)$  and  $1.964(5) \text{ \AA}$ ] are relatively long compared to  $\text{GeN}_3[\text{N}(\text{SiMe}_3)_2][\text{NPh}(\text{SiMe}_3)_2]$ , (8), [ $1.869(4) \text{ \AA}$ ], but are similar to those of the octahedral porphyrin complex,  $\text{Ge}(\text{tptp})(\text{N}_3)_2$  (tptp = 5,10,15,20-tetra-*p*-tolylporphyrinate), (9) [ $1.963(4) \text{ \AA}$ ]. Interestingly, the azide ligands of (9) more closely resemble canonical form (3) than (2) or (1) [N(1)–N(2)  $1.160(8)$ , N(2)–N(3)  $1.154(13) \text{ \AA}$ ], while the azide ligand of (8) is more analogous to resonance form (1) [or (2)] than (3) [N(1)–N(2)  $1.211(7)$ , N(2)–N(3)  $1.144(8) \text{ \AA}$ ] based on the solid-state structural data. However, neither (8) nor (9) can be considered prototypical germanium azides for comparative purposes since, in addition to azide ligands, (8) contains three planar amido ligands, while (9) has an expanded germanium co-ordination sphere. The azide ligands in (6) are slightly bent,  $176.1$  and  $176.0^\circ$ , a common feature of Group 14 azides. It has been predicted that the energy required to bend the azide ligand about the central nitrogen is very low.<sup>15</sup> The co-ordination about Ge is distorted, with the Fe–Ge–Fe angle enlarged [ $127.4(1)^\circ$ ] over the tetrahedral angle and the N(1)–Ge–N(4) angle reduced [ $97.2(2)^\circ$ ]. These deviations from local tetrahedral geometry are similar to those observed<sup>16</sup> for  $[\{\text{Fe}(\text{CO})_2(\text{cp})\}_2\text{GeCl}_2]$ , (10), and consistent with predictions based on the steric demand of the germanium substituents and rehybridization of  $\text{X}_2\text{EY}_2$  systems according to Bent's rules.<sup>17</sup> The Fe–Ge distances in (6) are similar to those of (10). There appears to be no evidence for  $\text{N} \rightarrow \text{Ge } p_\pi \rightarrow d_\pi$  interactions based on these solid-state structural data.

In the solid-state structure of compound (7) the two azide ligands are related by a  $C_2$  axis of molecular symmetry. Comparison of the N(1)–N(2) and N(2)–N(3) distances within the azide ligands is consistent with a close resemblance to canonical form (3). All other examples of organometallic tin

**Table 1.** Summary of crystal data and the experimental details for the X-ray diffraction studies of compounds (6) and (7)\*

Compound	(6)	(7)
<i>M</i>	510.6	556.7
Crystal size (mm)	0.23 × 0.46 × 0.69	0.05 × 0.18 × 0.18
<i>T</i> /°C	20	20
<i>a</i> /Å	8.155(2)	17.375(3)
<i>b</i> /Å	8.426(2)	7.573(2)
<i>c</i> /Å	15.374(3)	14.944(3)
$\alpha$ /°	101.76(3)	
$\beta$ /°	94.29(3)	113.34(3)
$\gamma$ /°	117.80(3)	
<i>V</i> /Å <sup>3</sup>	897.2(4)	1 805.5(7)
<i>D<sub>c</sub></i> /g cm <sup>-3</sup>	1.890	2.048
<i>F</i> (000)	504	1 080
<i>Z</i>	2	4
Space group	<i>P</i> $\bar{1}$	<i>C</i> 2/ <i>c</i>
Crystal system	Triclinic	Monoclinic
Reflections collected	7 022	3 681
Reflections used [ <i>I</i> > 3σ( <i>I</i> )]	3 041	1 663
2θ range/°	2.0–52.0	2.0–50.0
μ/mm <sup>-1</sup>	3.272	2.998
<i>R</i>	0.0369	0.0377
<i>R'</i>	0.0400	0.0612

\* Details in common: Radiation Mo-*K*<sub>α</sub> (λ = 0.710 69 Å), weighting scheme  $w^{-1} = \sigma^2(F) + 0.035 F^2$ .

**Figure 2.** An ORTEP plot of compound (7) showing the atom numbering scheme

azides structurally characterized in the solid state to date are polymeric with bridging azide ligands and therefore of little use for comparative purposes. It is noteworthy, however, that the azide ligand of  $\text{SnMe}_3\text{N}_3$  is more analogous to canonical form (3) than (2) or (1).<sup>8</sup> A number of  $[\{\text{Fe}(\text{CO})_2(\text{cp})\}_2\text{SnX}_2]$  species have been structurally characterized, including  $\text{X} = \text{Cl}$ ,<sup>18</sup> (11),  $\text{NO}_2$ ,<sup>19</sup> (12),  $\text{Me}$ ,<sup>20</sup> (13),  $\text{cp}$ ,<sup>21</sup> (14), and  $\text{OSO}_2\text{Ph}$ ,<sup>22</sup> (15). The deviation from tetrahedral co-ordination environment about tin and the Sn–Fe bond length are both similar to those of (11). The Fe–Sn bond lengths in (13) and (14) are significantly longer than those of (7) and (11) presumably as a result of inductive effects. The Sn–N bond distances are comparable to those expected for a single bond based on the sum of covalent radii for Sn and N.<sup>23</sup>

**Solid-state and Solution Spectral Data.**—There are six fundamental i.r.-active vibrations of organometallic azides if the moiety to which the azide is attached is considered a single site,<sup>3b</sup> but all six have never been simultaneously observed. The

**Table 2.** Atomic co-ordinates ( $\times 10^4$ )

Atom	<i>x</i>	<i>y</i>	<i>z</i>
<b>(a) Compound (6)</b>			
Ge	2 795(1)	2 295(1)	2 478(1)
N(1)	494(5)	1 379(6)	1 597(3)
N(2)	608(5)	1 897(6)	918(3)
N(3)	608(7)	2 323(7)	261(3)
N(4)	2 702(6)	4 402(5)	3 255(3)
N(5)	1 516(7)	4 082(6)	3 692(3)
N(6)	463(11)	3 865(8)	4 147(5)
Fe(1)	2 083(1)	24(1)	3 267(1)
C(1)	3 624(7)	−983(7)	3 901(3)
C(2)	2 297(7)	−925(7)	4 415(3)
C(3)	2 735(7)	935(8)	4 682(3)
C(4)	4 286(7)	2 006(7)	4 349(3)
C(5)	4 857(6)	849(7)	3 859(3)
C(6)	1 530(6)	−1 619(6)	2 237(3)
O(1)	1 163(5)	−2 739(5)	1 574(2)
C(7)	−208(6)	−284(6)	3 179(3)
O(2)	−1 721(4)	−518(5)	3 140(2)
Fe(2)	5 437(1)	3 630(1)	1 815(1)
C(8)	6 830(7)	3 664(7)	714(3)
C(9)	4 890(7)	2 396(7)	422(3)
C(10)	4 361(7)	1 026(7)	874(3)
C(11)	5 995(8)	1 436(7)	1 469(3)
C(12)	7 529(7)	3 089(7)	1 364(3)
C(13)	6 749(6)	4 844(6)	2 927(3)
O(3)	7 613(5)	5 646(5)	3 642(2)
C(14)	4 872(6)	5 379(6)	1 720(3)
O(4)	4 565(5)	6 515(5)	1 629(3)
<b>(b) Compound (7)</b>			
Sn	0	1 477(1)	2 500
N(1)	−230(3)	−488(9)	3 411(4)
N(2)	262(3)	−1 067(7)	4 090(4)
N(3)	729(5)	−1 686(14)	4 756(6)
Fe	−1 389(1)	2 946(1)	1 630(1)
C(1)	−1 825(3)	838(7)	1 283(3)
O(1)	−2 136(2)	−511(5)	1 043(3)
C(2)	−1 142(3)	3 238(7)	593(3)
O(2)	−1 003(3)	3 450(6)	−73(3)
C(3)	−1 658(6)	3 518(8)	2 847(5)
C(4)	−1 060(5)	4 623(10)	2 857(6)
C(5)	−1 328(6)	5 574(9)	2 032(8)
C(6)	−2 182(6)	5 074(11)	1 462(5)
C(7)	−2 368(4)	3 783(10)	2 007(6)

most commonly observed i.r. bands for azide ligands are the asymmetric stretch (2 150–1 950  $\text{cm}^{-1}$ ), the symmetric stretch (1 350–1 250  $\text{cm}^{-1}$ ), and a bend (700–600  $\text{cm}^{-1}$ ). The asymmetric stretch generally has the highest intensity and has been unambiguously assigned for compounds (6) and (7). Based on the X-ray structural data discussed above, both (6), *C*<sub>1</sub> molecular symmetry, and (7), *C*<sub>2</sub> molecular symmetry, are expected to exhibit four i.r.-active  $\nu(\text{CO})$  stretches and two  $\nu_{\text{asym.}}(\text{N}_3)$  stretches. These bands are observed, the positions of  $\nu_{\text{asym.}}(\text{N}_3)$  for (6) being 2 087 and 2 065  $\text{cm}^{-1}$  and for (7), 2 088 and 2 073  $\text{cm}^{-1}$  in the solid state. The  $\nu_{\text{asym.}}(\text{N}_3)$  stretches for  $\text{GeMe}_2(\text{N}_3)_2$  were observed at 2 126 and 2 105  $\text{cm}^{-1}$ .<sup>24</sup> The i.r. spectra of (6), (7),  $[\{\text{Fe}(\text{CO})_2(\text{cp})\}_2\text{GeBr}_2]$ , (16), and  $[\{\text{Fe}(\text{CO})_2(\text{cp})\}_2\text{SnCl}_2]$ , (11), were recorded in *C*<sub>6</sub>*D*<sub>6</sub> solution, and the data obtained in the  $\nu_{\text{asym.}}(\text{N}_3)$  and  $\nu(\text{CO})$  regions are in Table 5 and shown in Figure 3. It has previously been demonstrated that, in solution, (11) and (12) exhibit four  $\nu(\text{CO})$  bands with intensities consistent with point group symmetry *C*<sub>1</sub>,<sup>25</sup> although *C*<sub>2</sub> symmetry was unambiguously established in the solid state in both cases. The decrease in intensities of the  $\nu(\text{CO})$  bands of (16) and (11) with decreasing energy observed

**Table 3.** Relevant bond lengths (Å) for compounds (6) and (7)

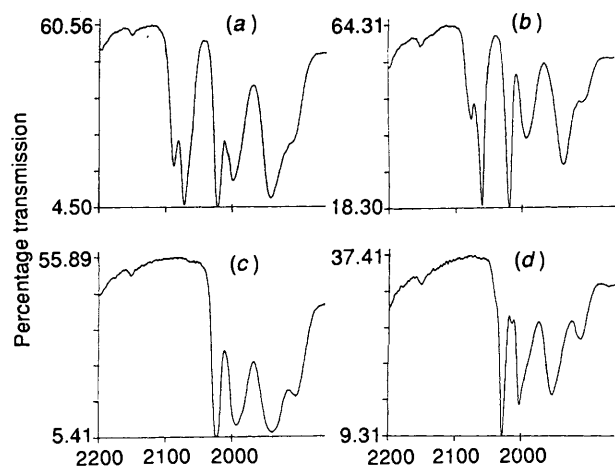
(6)				(7)	
Ge-N(1)	1.948(4)	Ge-N(4)	1.964(5)	Sn-N(1)	2.158(7)
Ge-Fe(1)	2.342(1)	Ge-Fe(2)	2.342(1)	Sn-Fe	2.504(1)
N(1)-N(2)	1.204(6)	N(4)-N(5)	1.178(7)	N(1)-N(2)	1.126(7)
N(2)-N(3)	1.139(7)	N(5)-N(6)	1.121(10)	N(2)-N(3)	1.108(9)
Fe(1)-C(1)	2.097(7)	Fe(2)-C(8)	2.105(6)	Fe-C(3)	2.094(10)
Fe(1)-C(2)	2.109(6)	Fe(2)-C(9)	2.094(4)	Fe-C(4)	2.114(8)
Fe(1)-C(3)	2.089(4)	Fe(2)-C(10)	2.097(5)	Fe-C(5)	2.069(7)
Fe(1)-C(4)	2.098(4)	Fe(2)-C(11)	2.080(7)	Fe-C(6)	2.070(9)
Fe(1)-C(5)	2.097(5)	Fe(2)-C(12)	2.090(7)	Fe-C(7)	2.091(9)
Fe(1)-C(6)	1.745(4)	Fe(2)-C(13)	1.763(4)	Fe-C(1)	1.755(5)
Fe(1)-C(7)	1.752(5)	Fe(2)-C(14)	1.766(6)	Fe-C(2)	1.779(6)
C(6)-O(1)	1.149(5)	C(13)-O(3)	1.140(5)	C(1)-O(1)	1.144(6)
C(7)-O(2)	1.150(6)	C(14)-O(4)	1.126(8)	C(2)-O(2)	1.124(8)

**Table 4.** Relevant bond angles (°) for compounds (6) and (7)

(6)				(7)	
N(1)-N(2)-N(3)	176.1(4)	N(4)-N(5)-N(6)	176.0(5)	N(1)-N(2)-N(3)	177.5(8)
N(1)-Ge-N(4)	97.2(2)	Fe(1)-Ge-Fe(2)	127.4(1)	N(1)-Sn-N(1)	92.8(4)
N(1)-Ge-Fe(1)	105.1(1)	N(4)-Ge-Fe(1)	107.8(1)	Fe-Sn-Fe	127.2(1)
N(1)-Ge-Fe(2)	109.8(1)	N(4)-Ge-Fe(2)	105.5(1)	N(1)-Sn-Fe	111.1(1)
Ge-N(1)-N(2)	119.0(3)	Ge-N(4)-N(5)	118.4(3)	Sn-N(1)-N(2)	125.0(5)

**Table 5.** Stretching frequencies (cm<sup>-1</sup>)  $\nu(\text{CO})$  and  $\nu_{\text{asym}}(\text{N}_3)$  for the complexes  $[\{\text{Fe}(\text{CO})_2(\text{cp})\}_2\text{EX}_2]$ 

Compound	E	X	$\nu_{\text{asym}}(\text{N}_3)$	$\nu(\text{CO})$
(6)	Ge	N <sub>3</sub>	2 091, 2 073	2 023, 2 000, 1 969, 1 955
(16)	Ge	Br		2 030, 2 005, 1 978, 1 957
(7)	Sn	N <sub>3</sub>	2 075, 2 060	2 019, 1 997, 1 969, 1 955
(11)	Sn	Cl		2 024, 1 997, 1 969, 1 952

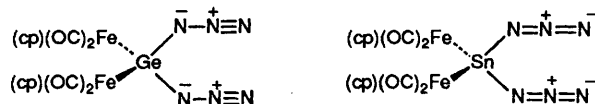
**Figure 3.** Infrared spectra of compounds (6) (a), (7) (b), (11) (c), and (16) (d) in the  $\nu(\text{CO})$  and  $\nu_{\text{asym}}(\text{N}_3)$  stretching region ( $\text{C}_6\text{D}_6$  solution)

here is consistent with expectations based on  $C_1$  symmetry as reported previously for similar compounds.<sup>25</sup> The alternating  $\nu(\text{CO})$  band intensities, however, of (6) and (7) are consistent with  $C_s$  symmetry in solution (on the i.r. time-scale) and are more characteristic of alkyl-substituted derivatives such as  $\text{GeMe}_2\{\text{Fe}(\text{CO})_2(\text{cp})\}_2$ . This is corroborated by the <sup>13</sup>C n.m.r.

data; compounds (6) and (7) exhibit only one type of carbonyl resonance at room temperature (on the n.m.r. time-scale). The two  $\nu_{\text{asym}}(\text{N}_3)$  bands exhibited by (6) and (7) are in a region characteristic of canonical form (3). The lower  $\nu_{\text{asym}}(\text{N}_3)$  stretches for (7), compared to (6), are probably a result of the higher mass of tin compared to germanium. The  $\nu_{\text{sym}}(\text{N}_3)$  stretches are observed at 1 281 cm<sup>-1</sup> for (6) and 1 294 cm<sup>-1</sup> for (7), in solution. The <sup>119</sup>Sn n.m.r. chemical shift of (7) (+520.9 p.p.m.) is more shielded than that of  $[\{\text{Fe}(\text{CO})_2(\text{cp})\}_2\text{SnCl}_2]$  (+550.5 p.p.m.) probably as a result of the lower effective electronegativity of the azide ligand compared to chloride.

### Conclusion

From the solid-state structural data it appears that the canonical form adopted by the azide ligands of  $[\{\text{Fe}(\text{CO})_2(\text{cp})\}_2\text{Ge}(\text{N}_3)_2]$  is best represented by (1), while that adopted by  $[\{\text{Fe}(\text{CO})_2(\text{cp})\}_2\text{Sn}(\text{N}_3)_2]$  is best represented by canonical form (3), as shown below.\* Contributions of resonance form (2) of the valence-bond model to the structures



(6) and (7) seem inappropriate. The predictive utility of the  $\nu_{\text{asym}}(\text{N}_3)$  i.r. active stretching frequency for assigning valence-bond contributions of azide ligands is questionable and further studies are required. There appears to be no evidence for Ge-N or Sn-N  $\pi$  bonding, and the relatively short Fe-Ge and Fe-Sn bond lengths could be explained simply by inductive effects. However, other explanations are possible, for example the long

\* Conclusions derived from solid-state structural data should be treated with some caution due to 'molecular packing forces.' However, there is no evidence for any intermolecular interactions (i.e. less than the sum of the van der Waals radii) in the solid-state structures of (6) or (7).

Ge-N distance of (6) compared to (8), together with the relatively short Fe-Ge distance of (6),\* could be the result of more favourable Fe→Ge  $d_{\pi}$ → $d_{\pi}$  overlap than N→Ge  $p_{\pi}$ → $d_{\pi}$  overlap. Finally, as Group 14 is descended, the polarity of the E-N<sub>3</sub> bond increases, and the resemblance to ionic azide ligands is likely to become stronger. Ionic azides (e.g. N<sub>3</sub><sup>-</sup>) are linear and symmetrical with N-N bond distances of 1.16 Å.<sup>26</sup> Clearly, further structural studies of Group 14 azides are required to probe the valence-bond contributions. Organometallic Group 14 azides decompose either by complete loss of the azide ligand or by Curtius-type rearrangement.<sup>27</sup> Reactivity studies of compounds (6) and (7) are currently underway.

### Acknowledgements

We thank the Sandia University Research Program for financial support, Dr. D. Doughty for helpful discussions, Eva Quesnell for typing this manuscript, and the National Science Foundation Chemical Instrumentation programme for the purchase of a low-field n.m.r. spectrometer.

\* For example,  $[\{Fe(CO)_2(cp)\}_2Ge(CH_2CMeCMeCH_2)]$  exhibits a Fe-Ge bond length of 2.416(1) Å.<sup>10d</sup>

### References

- 1 S. Patai, 'The Chemistry of the Azido Group,' Wiley-Interscience, New York, 1972; E. F. V. Scriven, 'Azides and Nitrenes: Reactivity and Utility,' Academic Press, New York, 1984.
- 2 M. Kaftory, 'The Chemistry of Halides, Pseudohalides and Azides,' eds. S. Patai and Z. Rappoport, Wiley, New York, 1983.
- 3 (a) G. Bertrand, J.-P. Majoral, and A. Baccero, *Acc. Chem. Res.*, 1986, **19**, 17; (b) J. S. Thayer, *Organomet. Chem. Rev.*, 1966, **1**, 157.
- 4 S. S. Zigler, K. J. Haller, R. West, and M. S. Gordon, *Organometallics*, 1989, **8**, 1656.
- 5 S. S. Zigler, L. M. Johnson, and R. West, *J. Organomet. Chem.*, 1988, **341**, 187.
- 6 P. Pfeiffer, W. Maringele, M. Noltemeyer, and A. Meller, *Chem. Ber.*, 1989, **122**, 245.
- 7 R. Guillard, J.-M. M. Barbe, M. Boukhris, and C. Lecomte, *J. Chem. Soc., Dalton Trans.*, 1988, 1921.
- 8 R. Allman, R. Hohlfeld, A. Waskowska, and J. Lorberth, *J. Organomet. Chem.*, 1980, **353**, 192.
- 9 A. Gambaro, D. Marton, and G. Tagliavini, *J. Organomet. Chem.*, 1981, **57**, 210.
- 10 (a) D. Lei and M. J. Hampden-Smith, *J. Chem. Soc., Chem. Commun.*, 1989, 1211; (b) D. Lei, M. J. Hampden-Smith, E. N. Duesler, and J. C. Huffman, *Inorg. Chem.*, 1990, **29**, 795; (c) D. Lei, M. J. Hampden-Smith, and E. N. Duesler, *Polyhedron*, 1990, **9**, 1127; (d) G. Barsuaskas, D. Lei, M. J. Hampden-Smith, and E. N. Duesler, *Polyhedron*, 1990, **9**, 773.
- 11 D. F. Shriver and M. A. Drezdson, 'The Manipulation of Air-Sensitive Compounds,' 2nd edn., Wiley-Interscience, New York, 1986, p. 78-79.
- 12 A. J. Gordon and R. A. Ford, 'The Chemist's Companion,' Wiley, New York, 1972.
- 13 F. Bonati and G. Wilkinson, *J. Chem. Soc.*, 1964, 179.
- 14 M. D. Curtis and P. Woller, *Inorg. Chem.*, 1972, **11**, 431.
- 15 J. Roberts, *Chem. Ber.*, 1961, **94**, 273.
- 16 M. A. Bush and P. Woodward, *J. Chem. Soc. A*, 1967, 1833.
- 17 H. A. Bent, *Chem. Rev.*, 1961, **61**, 275.
- 18 J. E. Connor and E. R. Corey, *Inorg. Chem.*, 1967, **6**, 968.
- 19 B. P. Bir'yukov, Y. T. Strichkov, K. N. Anisimov, N. E. Kolobova, and V. V. Skripkin, *Chem. Commun.*, 1967, 750.
- 20 B. P. Bir'yukov, Y. T. Strichkov, K. N. Anisimov, N. E. Kolobova, and V. V. Skripkin, *Chem. Commun.*, 1968, 159.
- 21 B. P. Bir'yukov, Y. T. Strichkov, K. N. Anisimov, N. E. Kolobova, and V. V. Skripkin, *Chem. Commun.*, 1968, 1193.
- 22 R. F. Bryan and A. R. Manning, *Chem. Commun.*, 1968, 1220.
- 23 J. E. Huheey, 'Inorganic Chemistry, Principles of Structure and Reactivity,' 3rd edn, Harper and Row, Mill Valley, California, 1983.
- 24 J. Barrau, D. L. Bean, K. M. Welsh, R. West, and J. Michl, *Organometallics*, 1989, **8**, 2006.
- 25 N. Flitcroft, D. A. Harbourne, I. Paul, P. M. Tucker, and F. G. A. Stone, *J. Chem. Soc. A*, 1966, 1130.
- 26 N. N. Greenwood and A. Earnshaw, 'The Chemistry of the Elements,' Pergamon, Oxford, 1984; A. F. Wells, 'Structural Inorganic Chemistry,' 4th edn., Clarendon Press, Oxford, 1975.
- 27 K. M. Welsh, J. Michl, and R. West, *J. Am. Chem. Soc.*, 1989, **110**, 6689; H. Vancik, G. Raabe, M. J. Michalczyk, R. West, and J. Michl, *ibid.*, 1985, **107**, 4097; N. Wiberg, P. Karampatses, and C. Kim, *Chem. Ber.*, 1987, **120**, 1203; C. Guimon and G. Pfister-Guillonzo, *Organometallics*, 1987, **6**, 1387.

Received 1st March 1990; Paper 0/00947D